ISBN: 978-3-95450-247-9 ISSN: 2673-5490 doi: 10.18429/JACoW-IPAC2024-MOPC43

CORRECTION OF THE DETECTOR SOLENOID EFFECT IN THE HADRON STORAGE RING OF THE ELECTRON-ION COLLIDER*

V. S. Morozov†, Oak Ridge National Laboratory, Oak Ridge, TN 37831, USA
J. S. Berg, M. Blaskiewicz, A. Blednykh, C. Liu, H. Lovelace III, Y. Luo, D. Marx, C. Montag, S. Nagaitsev, S. Peggs, V. Ptitsyn, S. Tepikian, F. Willeke, H. Witte, and D. Xu,
Brookhaven National Laboratory, Upton, NY 11973, USA
T. Satogata, Jefferson Lab, Newport News, VA 23606, USA

Abstract

The Electron Ion Collider design strategy for reaching unprecedented luminosities and detection capabilities involves collision of flat bunches at a relatively large crossing angle. Effective head-on collisions are restored using crab cavities, which introduce a correlation of the particles' transverse coordinates with their longitudinal positions in the bunch, or crab dispersion. The collision geometry is further complicated by a tilt of the Electron Storage Ring plane with respect to that of the Hadron Storage Ring. In addition, the interaction point is placed inside the field of a detector solenoid. Reaching the design luminosity requires precise control of the 6D bunch distribution at the IP accounting for all of the aforementioned design features. This paper describes correction of the detector solenoid effect on the beam optics of the Hadron Storage Ring using a combination of local and global skew quadrupoles.

INTRODUCTION

The high-luminosity design of the Electron-Ion Collider (EIC) [1, 2] relies in part on collision of rather flat beams at its 6 o'clock Interaction Point (IP6). The necessary level of flatness is achieved by both asymmetric optics design and a large difference of the horizontal and vertical emittances. For detection purposes, IP6 is placed at the center of a 4 m long up-to 2 T detector solenoid [3]. The solenoid causes transverse coupling, which affects the bunch distribution at IP6 and tends to redistribute and equalize the transverse emittances. Therefore, transverse coupling must be compensated both locally at IP6 and globally for the entire ring.

A unique feature of the EIC is that the ion beam crosses the detector solenoid at a relatively large angle of 25 mrad necessitated by the detection requirements. The associated geometric luminosity loss is corrected using crab crossing – a bunch rotation at IP6 about the vertical axis. The rotation is induced by Crab Cavities (CCs) located at about $\pi/2$ horizontal betatron phase advance on both sides of IP6. This means that one needs to control the ion orbit and orientations of the interaction and crabbing planes at IP6.

An additional complication is that the plane of the electron ring is tilted with respect to the hadron ring to allow the two rings to cross without introducing vertical bends in the tunnel. This tilt translates into an effective 4 mrad rotation of the electron beam plane at IP6 [4], which must also be accounted for.

Simulations of the beam-beam interaction found [5] that precise control of the momentum and crabbing dispersions is required at IP6 to prevent emittance degradation.

The detector solenoid effects requiring compensation can be summarized as

1. IP position and interaction plane orientation,
2. Orientation of the crabbing plane,
3. Momentum dispersion,
4. Local and global transverse coupling.

Note that the solenoid has an impact on the proton polarization, but analysis of this effect is beyond the scope of this paper. The 275 GeV beam optics [6] with the solenoid switched on but not corrected is shown in Fig. 1.

CORRECTION OF SOLENOID EFFECTS

Closed Orbit and Interaction Plane

Since the ion beam goes through the solenoid at an angle to its axis, the solenoid field has a radial component with respect to the ion orbit. It results in a primarily vertical distortion of the closed orbit. The distortion is such that the beam offset at the center of the solenoid is nearly zero, while the orbit angle is not. This is effectively a rotation of the interaction plane, which needs to be compensated according to the detector requirements. In addition, the 4 mrad rotation of the electron beam plane must be accounted for.

Note that, depending on the solenoid field direction, the beam rotation induced by the solenoid either adds up with or partially cancels the electron ring tilt effect. Since the detector has to be capable of operating with both solenoid field orientations, below we focus on the more challenging case of addition of the two rotations.

We account for the electron plane tilt by considering the ion orbit in a reference frame locally rotated by 4 mrad about the longitudinal axis at IP6. We then require that the ion closed orbit is corrected at IP6 in this frame, $\vec{x}_{co} = \vec{0}$, and that the orbit distortion is localized to the interaction region (IR) area of IP6. These conditions are satisfied by two dual-plane correctors on each side of IP6. Their locations

* This manuscript has been authored in part by UT-Battelle, LLC, Brookhaven Science Associate, LLC, and Jefferson Science Associates, LLC under Contracts DE-AC05-00OR22725, DE-SC0012704, and DE-AC05-06OR23177 with the US Department of Energy (DOE).
† morozovvs@ornl.gov

ISBN: 978-3-95450-247-9 ISSN: 2673-5490 doi: 10.18429/JACoW-IPAC2024-MOPC43

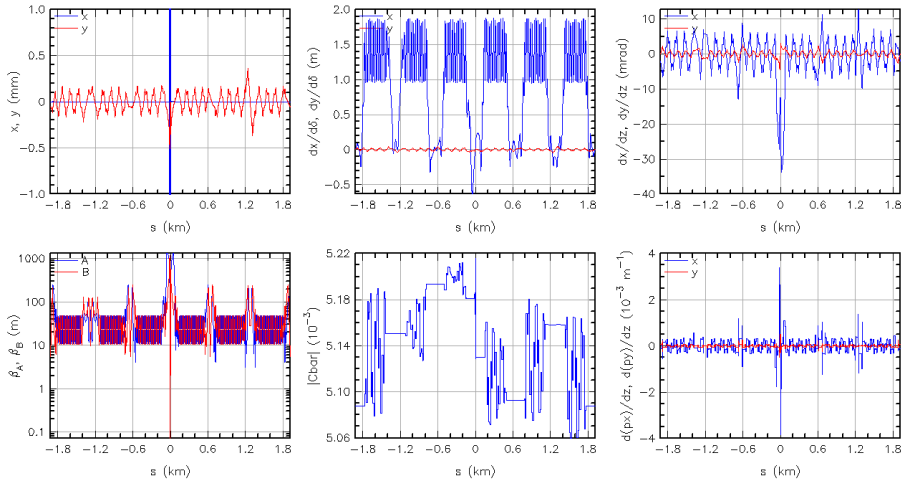

Figure 1: Horizontal (blue) and vertical (red) closed orbit coordinates (top left), β functions (bottom left), momentum dispersion components (top center), and components of the crab dispersion (top right) and its slope (bottom right) around the ring before correction of the detector solenoid. $|Cbar|$ (bottom center) is the determinant of the normalized coupling matrix $\bar{C}$.

are chosen considering their efficiency, space availability and engineering requirements. Their parameters assuming 275 GeV protons are listed in Table 1. Note that the corrector strengths scale proportionally to the solenoid strength, and the corresponding absolute fields are nearly independent of the beam energy. The corrected orbit is plotted in Fig. 2 (top left).

Table 1: Parameters of the dipole correctors for compensation of the orbit distortion caused by the detector solenoid.

Corrector #	s (m)	$\Delta x'$ (μrad)	$\Delta y'$ (μrad)
1	39.5	0	-8.2
2	15.0	0.3	5.1
3	-8.2	-0.8	8.1
4	-38.1	-0.6	-12.5

Crab Dispersion

The detector requirements are not compatible with placement of anti-solenoids in IR6. Coupling is corrected with skew quads. Since the largest crab dispersion is localized to the IR6 section between the CCs, that area allows for most efficient control of the vertical crab dispersion with skew quads. Limited variation of the betatron phase advance from IP6 to both CC sections precludes one from implementing the entire coupling compensation between IP6 and the CCs. Therefore, we place two local skew quads on each side of IP6 with the main goal of managing the vertical crab dispersion, while the remaining coupling effects are handled by the global skew quad families, as discussed below.

A CC imposes a horizontal kick $\Delta x'(z) = dx'/dz \cdot z$ on a passing bunch. To prevent its conversion into a vertical crab dispersion at IP6 $(dy/dz,\ dy'/dz)_{IP}$, the beam transport matrix $M^{CC\to IP6}$ between IP6 and the CC must satisfy

$$M_{32}^{CC\to IP6} = \left.\frac{dy}{dz}\right|_{IP} \Big/ \left.\frac{dx'}{dz}\right|_{CC} = 0,$$
$$M_{42}^{CC\to IP6} = \left.\frac{dy'}{dz}\right|_{IP} \Big/ \left.\frac{dx'}{dz}\right|_{CC} = 0. \qquad (1)$$

Two local skew quads on each side of IP6 are sufficient to satisfy the conditions of Eq. (1). Note that the horizontal crabbing dispersion is not completely closed in IR6 due to a deviation of the horizontal betatron phase advance between the CCs from 180°. This means that the vertical crabbing dispersion is not localized to IR6 after correction. The horizontal dispersion leaks outside of IR6 and is coupled into the vertical plane by the global skew quads around the ring. The local skew quads are the most efficient knobs for correction of the vertical crab dispersion at IP6 from all sources.

Vertical Momentum Dispersion and Transverse Coupling

Compensation of transverse coupling induced by a detector solenoid is a common task in many storage rings. Strategies for coupling correction with skew quads are straightforward [7–9]. In general, four independent knobs are needed to cancel four independent coupling coefficients and thus zero out both (2×2) off-diagonal blocks of a (4×4) transport matrix. Optimal placement of skew quads in terms of the horizontal and vertical betatron phase advance $(\Delta\mu_x,\ \Delta\mu_y)$ between them can be specified as

$$(\Delta\mu_x,\ \Delta\mu_y): \quad (\pi/2, 0),\ (\pi/2, \pi/2),\ (0,0),\ \text{and } (0,\pi/2)\ (\text{mod } \pi). \qquad (2)$$

Control of the vertical momentum dispersion at IP6 requires two additional skew quad knobs at dispersive locations.

In practice, it is not always possible to place skew quads at the optimal orthogonal locations specified by Eq. (2). We

ISBN: 978-3-95450-247-9 ISSN: 2673-5490 doi: 10.18429/JACoW-IPAC2024-MOPC43

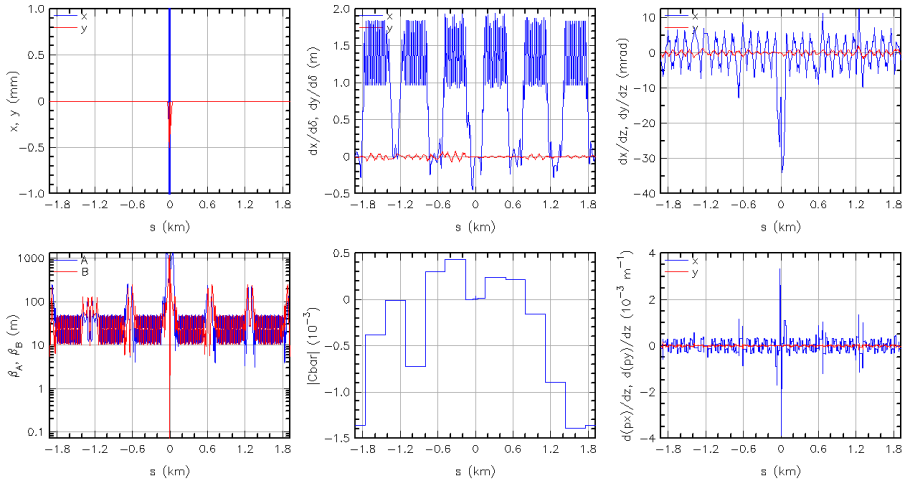

Figure 2: Horizontal (blue) and vertical (red) closed orbit coordinates (top left), β functions (bottom left), momentum dispersion components (top center), and components of the crab dispersion (top right) and its slope (bottom right) around the ring after correction of the detector solenoid. $|Cbar|$ (bottom center) is the determinant of the normalized coupling matrix $\bar{C}$.

found that compensation of the vertical crabbing dispersion with the local skew quads generates large residual transverse coupling because the local quads are placed at high-β locations. We explored the option of correcting the residual coupling locally with additional skew quads in IR6. However, the extra quads can only be placed at locations with relatively small β functions. This then yields impractically high quad strength requirements.

It is more efficient to compensate the residual coupling globally. Therefore, we adopt RHIC's 12 existing global skew quad families, 2 per sextant of the Hadron Storage Ring (HSR) [10]. Each family consists of 3 to 5 quads with an independent power supply. We initially model each family by a single thin quad placed near one of the family's quads. While not perfectly orthogonal, the families span sufficiently wide range of betatron phase advance conditions to provide the necessary knobs for efficient correction of the coupling effects.

Since the number of knobs available to us is greater than the number of constraints, we ensure the optimal use of the skew quad strengths by first numerically calculating a response matrix and then finding its Moore-Penrose inverse. It provides a minimum-norm solution for the quad strengths. It is worth noting that, due to the ambiguity of parameterizing the transport matrix in terms of the momentum and crab dispersions, we specify the constraints in terms of the beam Σ matrix elements, e.g., $dx/d\delta \equiv \sigma_{x\delta}/\sigma_{\delta\delta}$. The linear solution is refined numerically. The corrected optics is shown in Fig. 2. The locations and strengths of the local and global skew quads are indicated in Fig. 3. Figure 3 corresponds to the scenario requiring the highest quad strengths.

CORRECTION OF PLANAR OPTICS

Figures 1 and 2 indicate that the solenoid and its correction do not have a significant impact on the planar optics

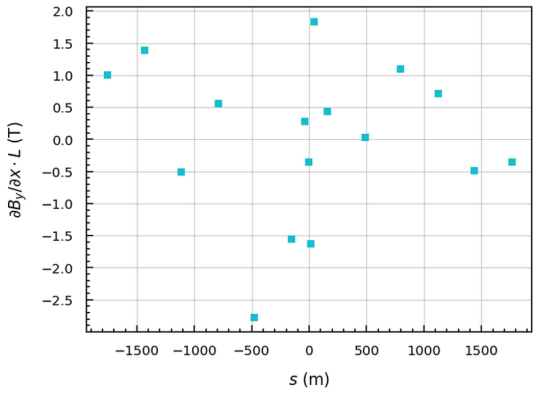

Figure 3: Integrated strengths of the local and global skew quads versus their positions in the HSR.

around the ring. Nevertheless, the optics at IP6 is somewhat modified and needs to be restored to its design parameters. The β functions at IP6 are adjusted by small modification of the strengths on two final focusing quads on each side of IP6. The relative change is of the order of $< 10^{-3}$. Control of the horizontal crab dispersion and its slope is accomplished by tuning the voltage of the forward and rear crab cavities. Since the momentum dispersion is relatively small in IR6, it is controlled at IP6 by invoking two existing straight quad families in the adjacent arcs where a large horizontal dispersion provides a good leverage over the dispersion in IR6.

CONCLUSION

A scheme for full control of the detector solenoid coupling effects in EIC's HSR has been developed. Our analysis of the compensation problem led us to a solution involving both local and global skew quads. We are currently working on the development of an experimental procedure for implementation of the correction in operation.

ISBN: 978-3-95450-247-9 ISSN: 2673-5490 doi: 10.18429/JACoW-IPAC2024-MOPC43

REFERENCES

[1] F. Willeke, "Electron Ion Collider Conceptual Design Report 2021", doi:10.2172/1765663

[2] C. Montag *et al.*, "The EIC accelerator – design highlights and project status", presented at the IPAC'24, Nashville, TN, USA, May 2024, paper MOPC67, this conference.

[3] H. Witte *et al.*, "Progress on the design of the interaction region of the Electron-Ion Collider EIC", presented at the IPAC'24, Nashville, TN, USA, May 2024, paper MOPC75, this conference.

[4] D. Xu *et al.*, "Beam-Beam Interaction for Tilted Storage Rings", in *Proc. IPAC'22*, Bangkok, Thailand, Jun. 2022, pp. 1968–1971. doi:10.18429/JACoW-IPAC2022-WEPOPT049

[5] Y. Luo *et al.*, "Tolerances of Crab Dispersion at the Interaction Point in the Hadron Storage Ring of the Electron-Ion Collider", in *Proc. NAPAC'22*, Albuquerque, NM, USA, Aug. 2022, pp. 12–15. doi:10.18429/JACoW-NAPAC2022-MOYD5

[6] Y. Luo *et al.*, "Wide range tune scan for the hadron storage ring of the Electron-Ion Collider", presented at the IPAC'24, Nashville, TN, USA, May 2024, paper MOPC79, this conference.

[7] S. Peggs, "The projection approach to solenoid compensation", CERN/SPS/82-2 (1982).

[8] Y. Nosochkov, Y. Cai, J. Irwin, M. Sullivan, and E. Forest, "Detector Solenoid Compensation in the PEP-II B-Factory", in *Proc. PAC'95*, Dallas, TX, USA, May 1995, paper RAA25, pp. 585–587.

[9] D. Sagan and D. Rubin, "Linear analysis of coupled lattices", Phys. Rev. ST Accel. Beams **2**, 074001 (1999). doi:10.1103/PhysRevSTAB.2.074001

[10] Y. Luo *et al.*, "Global betatron coupling compensation for the hadron storage ring of the Electron-Ion Collider", presented at the IPAC'24, Nashville, TN, USA, May 2024, paper MOPC80, this conference.